Investigation of Various Phenomena in Nuclear Physics using $Tl-204$, $Co-60$, $Po-210$, and $Sr-90$ Radioactive Sources

Yotam Granov* and Ofir Shukrun†

June 2023

Abstract

In this work, we used a Geiger counter in order to investigate various phenomena from the world of nuclear physics. Some of the experiments involved include plateau experiments, background measurements, statistical profiles, inverse-squared law verification, alpha decay investigation, and beta decay investigation (especially with respect to mass attenuation).

Contents

*ID: 211870241, Email: yotam.g@campus.technion.ac.il
†ID: 206228249, Email: ofir-s@campus.technion.ac.il

1 Introduction

1.1 Experimental Setup

As seen in Figure (1), the experimental setup for this work relied on an ST-360 counter, GM tube that is connected to it, radioactive sources and absorbers.

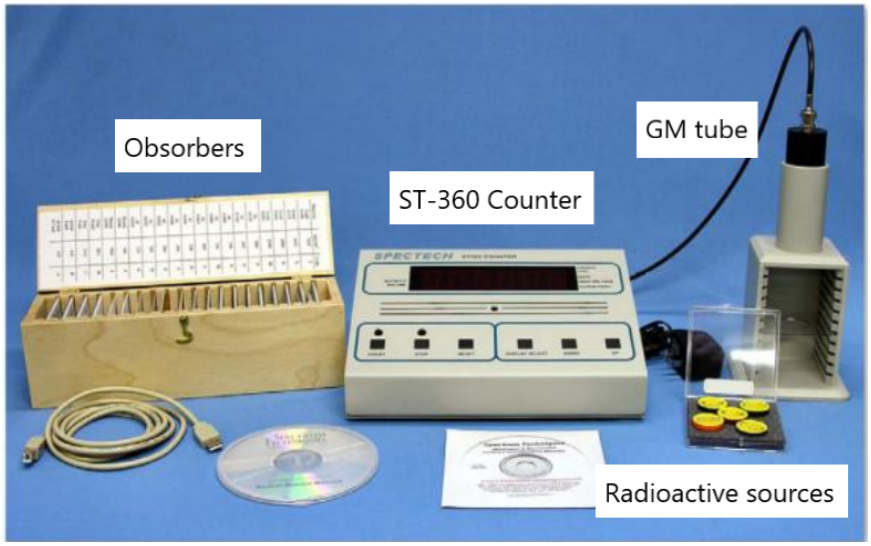

Figure 1: Experimental setup

1.2 Radioactive Materials

Radioactive materials are materials that have an unstable nucleus and thus emit particles such as alpha, beta and gamma. This radiation can be measured using Geiger counter: a gaseous ionization detector and uses the ionization process for gases in order to get signal from the radiation. In our beta experiments we chose to use $Tl - 204$ for our main source since it has a higher decay rate than the others.

1.3 Statistics of Counting & Background Radiation Measurement

We would like to know if probability of counting the radioactive material is given by Poisson or Gaussian distribution. The mean value is

$$\bar{n} = \frac{1}{m}\sum_{i=1}^{m} n_i$$

The probability of n events during a terminal time is

$$P_P(n) = \frac{\lambda^n e^{-\lambda}}{n!}$$

We counted the number of events and divided it by the time we measured to get the average events per second. In this case the mean and standard deviation are

$$\mu_P = \lambda,\ \sigma_P = \sqrt{\lambda}$$

We will obtain the third moment of a distribution

$$K_3 = \frac{1}{m-1}\sum_{i=1}^{m}(n_i - \bar{n})^3 \tag{1}$$

which will be different for each one of the distributions:

$$K_3^P = \lambda,\ K_3^G = 0$$

This will help us to distinguish between the two and determine the probability of the events. According to probability theory, in large numbers of events the central limit theorem states that for independent variables, the distribution will be normal even if each one of the random variables doesn't relate to normal distribution. Therefore, we can conclude that both graphs will be the same.

1.4 Inverse-Squared Law

For a spherical radiation, the intensity on a sphere is given by

$$I = \frac{P}{A}$$

where P is the power and $A = 4\pi r^2$ is the spherical surface area that the power acts on. In which case

$$I \propto \frac{1}{r^2}$$

gives us the inverse square law. Since the source is smaller then the detector we can assume that it emits the radiation spherically in the direction of the detector. Since there is a gap with width a between the top of the box and the detector we can write that

$$r = x + a$$

where x is the distance to the top of the box. We will find a using the inverse square law.

1.5 Range of Alpha Particles

Alpha particle are a nucleus of an Helium H^{2+}. they are characterize by short distance range since they are relatively heavy and slow, making their penetration power low. That is why they can't even pass through a piece of paper. We put the alpha source on tiny blocks in different heights until there was almost no events in the detector. That way we figured out the distance of the alpha trails.

1.6 Absorption of Beta Particles and Beta Decay Energy

Beta particles $\beta^{\pm}$ are positron and electron respectively. The beta decay process is given by

$$n \to p + \beta^- + \bar{\nu_e}$$

Meaning that the neutron is decaying to proton, electron and an anti-electron neutrino. The proton stays in the nucleus while the electron and the antineutrino emit. Since our detector can only detect ionizing radiation, we won't get any signal from the antineutrino. In addition, the emitted energy is distributed between the electron and the antineutrino.

In our experiment we used beta sources $Tl - 204$ and $Sr - 90$ and put various absorbers in order to absorb their radiation. This was in order to compare the spectra of the sources and state the thickness of the first absorber to absorb all of the energy of the betas.

2 Results & Analysis

2.1 Plateau Experiment

In the first part of the experiment, we record the number of counts measured by the Geiger counter in a period of 5 seconds for a range of voltage values between $500[V]$ and $1200[V]$ (in jumps of $5[V]$), where the source is thallium-204.

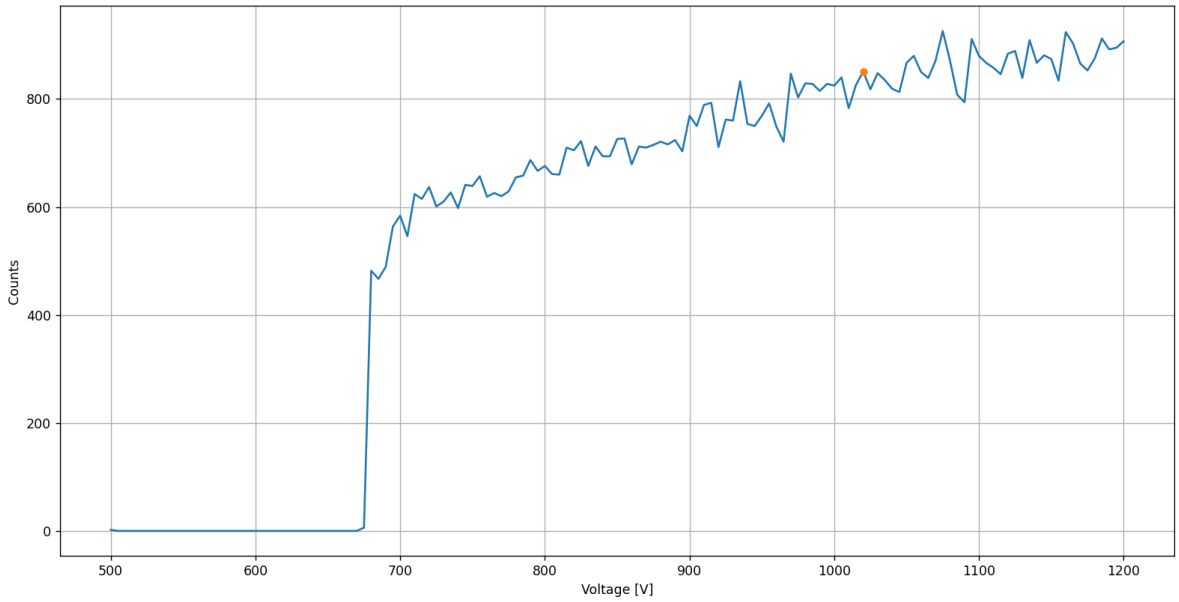

Figure 2: Plateau experiment results with $Tl - 204$

In Figure (2), we see that there is a big jump in the number of counts at $680[V]$, and we determine that the plateau (i.e. steady state results) is closer to $1020[V]$ (marked by a red dot in the figure).

2.2 Statistics & Background Measurements

In order to correct our subsequent results such that they take into account the presence of background radiation in the laboratory, we measured the radiation rate without any radioactive sources placed under the Geiger counter. We saw 46 counts over 100 seconds, and thus our background radiation rate is:

$$R_b = \frac{46}{100} = 0.46[\frac{counts}{sec}]$$

Then, we added a cobalt-60 source underneath the Geiger counter on the furthest shelf (at a distance of $94[mm]$ away). We measured the radiation across 10 trials, each of 1 second duration, and obtained $\bar{n} = 5.2$. We then calculated

$$m = 150 \cdot \bar{n} = 780$$

and then conducted m measurements (trials of 1 second duration each). From this new batch of measurements, we obtained $\bar{n} = 5.762 \pm 0.084$. Using Equation (1) we obtain $K_3 = 6.099 \pm 2.087$, and seeing that K_3 is much closer in value to $\bar{n}$ than it is to zero, we can conclude that the distribution is in fact Poissonian. Figure (3) shows a histogram of the data recorded in this experiment, as well as a Poissonian model of the distribution which matches the data quite well.

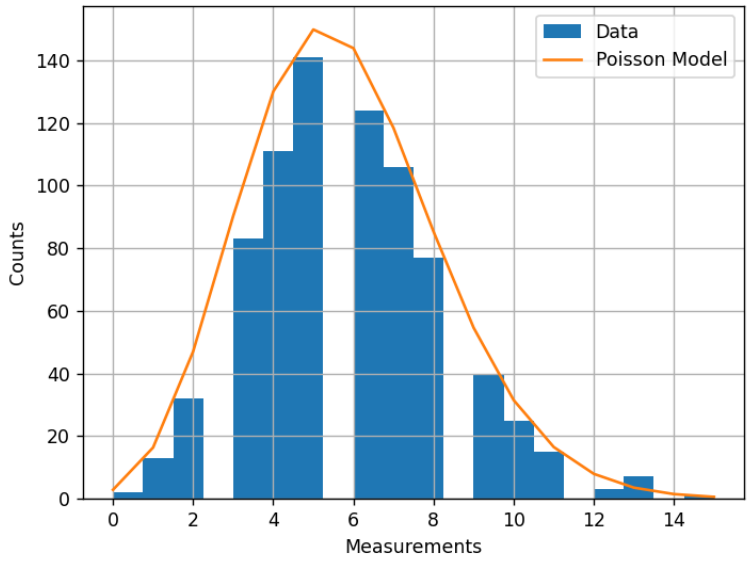

Figure 3: Histogram showing the measurements for $Co-60$ decay, along with a corresponding Poisson model

2.3 Inverse-Squared Law

In this part of the experiment, we place a thallium-204 beta source under the Geiger counter and vary its distance from the counter in order to investigate the inverse-squared law for radiation. In order to assess the validity of this law, we will find a function of the background-corrected radiation rate $(R - R_b)$ that is linear with the distance, such that a simple linear regression will suffice for our analysis. It turns out that $\frac{1}{\sqrt{R-R_b}}$ is the necessary function, as can be seen below:

$$R - R_b = \frac{b}{(x+a)^2} \rightarrow \frac{1}{\sqrt{R-R_b}} = \frac{1}{\sqrt{b}} \cdot x + \frac{a}{\sqrt{b}}$$

Thus, we can fit $\frac{1}{\sqrt{R-R_b}}$ as a linear regression in terms of the distance x in order to obtain a and b.

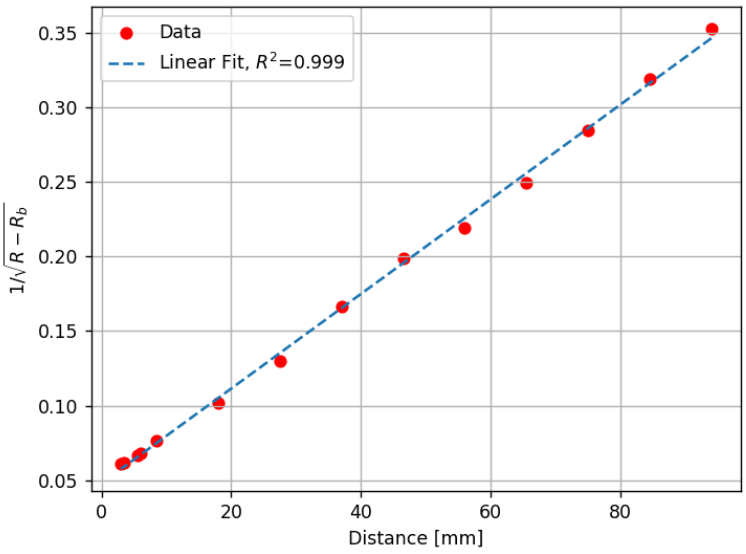

Figure 4: Linear model relating radiation rate and distance for a $Tl-204$ beta source

This linear regression can be seen in Figure (4), and it gives us values of $a = 15.074[mm]$ and $b = 99041.872$. We thus obtain the following inverse-squared relation for this source:

$$R - R_b = \frac{99041.872}{(x + 15.074)^2} \tag{2}$$

Figure (5) compares the model from Equation (2) to the actual data we obtained. It's clear that the model fits the data sufficiently well, and the inverse-squared law for radiation indeed holds.

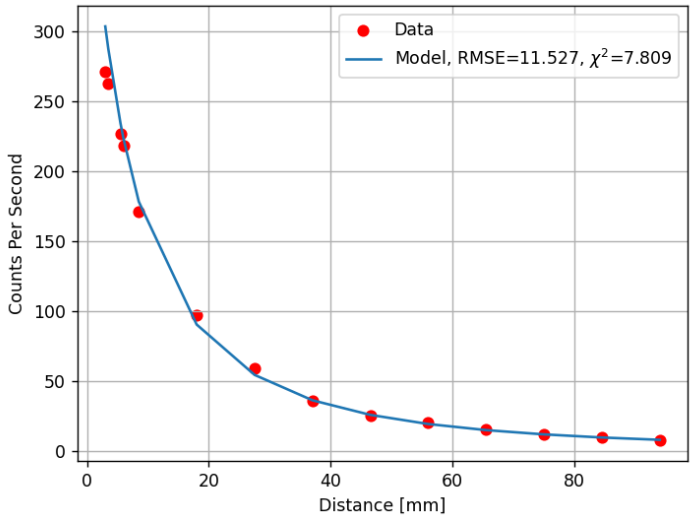

Figure 5: Model and data for radiation rate vs. distance, for a $Tl - 204$ beta source

2.4 Alpha Decay

In this part of the experiment we used polonium-210 to produce alpha particles, which lose most of their energy through particle collisions as they travel through air. We varied the distance of the alpha source from the detector, and thus obtained the data points shown in Figure (6) - we adjusted these data points to account for the background rate and a-factor previously obtained.

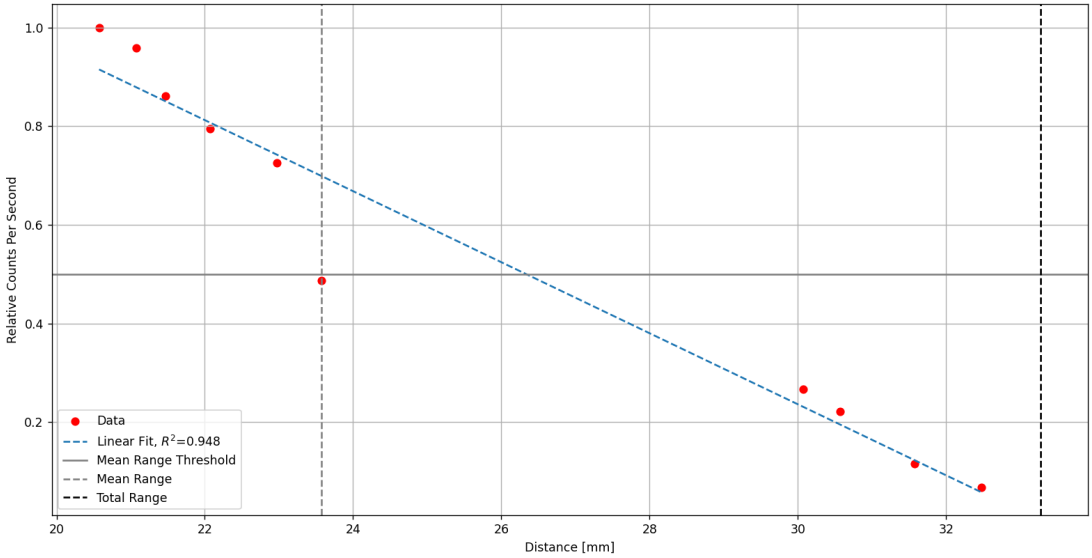

Figure 6: Relative radiation rate vs. distance, for a $Po - 210$ alpha source

Using linear regression (with a weakly conclusive R^2 value of 0.948) we were able to extrapolate the data until the point where the count rate is zero, which occurs at $33.279[mm]$ (we call this the total or extrapolated range). We also observed that the relative count rate dropped to 0.5 (or half the maximal count rate) at around $23.574[mm]$, and we take this to be the alpha particle's mean range in air. The expected mean range is $2.5[cm]$ and the expected total range is $3.4[cm]$, thus giving χ^2 values of $8.136 \cdot 10^{-3}$ and $1.531 \cdot 10^{-3}$, respectively.

From [3], we see that the mean range r_{mean} (in cm) can be related to the alpha particle's energy E (in MeV) using the following empirical relations:

$$r_{mean} = \begin{cases} 0.56E, & E < 4[MeV] \\ 1.24E - 2.62, & 4 < E < 8[MeV] \end{cases}$$

We observe that the latter energy range is more appropriate, and thus obtain the energy of the alpha particles in our experiment:

$$E = \frac{r_{mean} + 2.62}{1.24} = 4.014[MeV]$$

Figure (7) shows the expected values for the alpha's energy as a function of its mean range. It tells us that the energy of these particles should be roughly $3.9[MeV]$, and thus we have a χ^2 value of $3.333 \cdot 10^{-3}$ for our result.

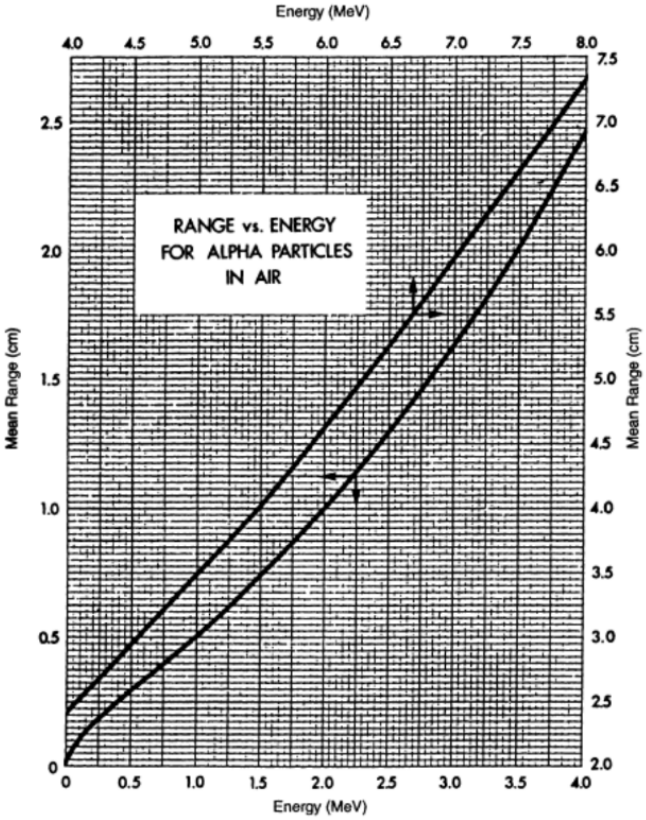

Figure 7: Range-energy plot for alpha particles in air at $15°C$ and $760[mmHg]$ pressure [1]

2.5 Beta Decay

In this part of the experiment, we investigate the effect of mass attenuation on the measurements of radiation due to beta decay for thallium-204 and strontium-90 sources (which are placed at a

distance of 27.5$[mm]$ from the detector). Using the Beer-Lambert Law, we can model the count rate for beta decay as a function of the density using an exponential function, which we can then apply the natural logarithm to in order to obtain a linear relation between a function of the count rate and the density. Such a process can be seen below:

$$R(t) = R_0 e^{-\mu t} \rightarrow ln(R) = ln(R_0) - \mu t$$

By plotting $ln(R)$ as a function of t (as we do in Figure (8) for $Tl - 204$ and $Sr - 90$) and applying a linear regression to the result, we can take the negative of the fitted slope in order to obtain the mass attenuation coefficient μ.

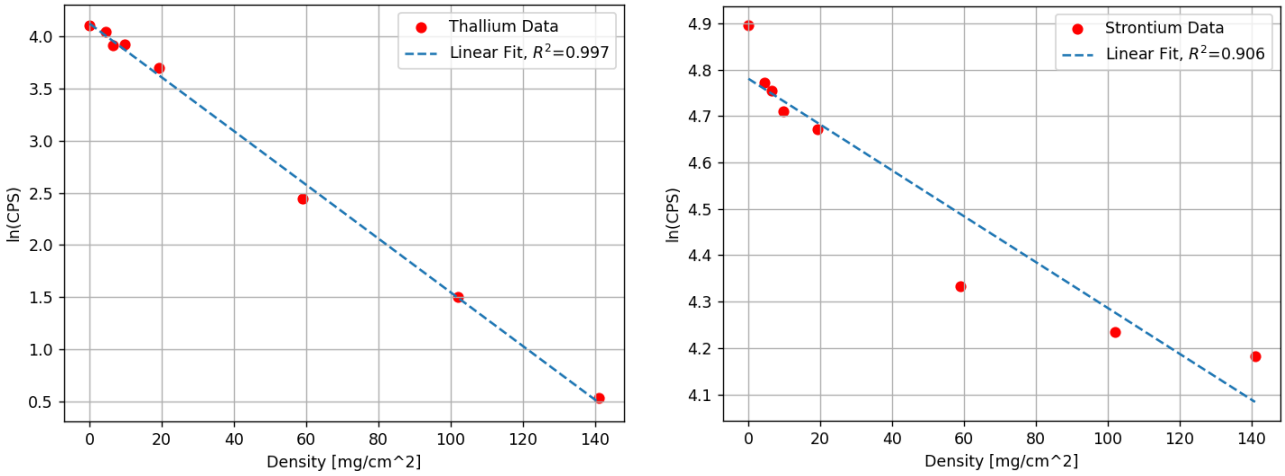

Figure 8: Natural log of the count rate vs. matter density for $Tl - 204$ (left) and $Sr - 90$ (right)

We obtained mass attenuation values of $\mu_{Tl} = 0.026[\frac{cm^2}{mg}]$ and $\mu_{Sr} = 0.005[\frac{cm^2}{mg}]$, noting that the linear fit was much stronger in the case of thallium than in the case of strontium. We then found the range r for each source by setting $R = R_b$ and solving for t:

$$R_b = R_0 e^{-\mu r} \rightarrow r = \frac{ln(R_0) - ln(R_b)}{\mu}$$

and obtained $r_{Tl} = 190.089[\frac{mg}{cm^2}]$ and $r_{Sr} = 1124.787[\frac{mg}{cm^2}]$.

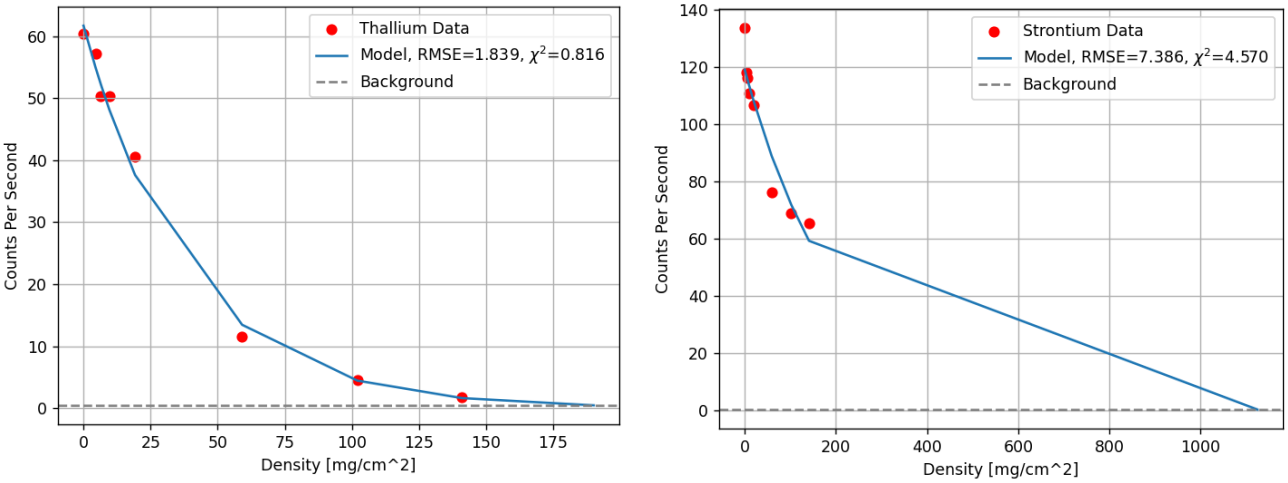

Figure 9: Count rate vs. matter density for $Tl - 204$ (left) and $Sr - 90$ (right)

From [3], we see that the range r (in $\frac{mg}{cm^2}$) can be related to the beta particle's energy E (in MeV) using the following empirical relation (since $r < 1200[\frac{mg}{cm^2}]$ for both):

$$ln(E) = 6.63 - 3.2376 \cdot \sqrt{10.2146 - ln(r)}$$

Thus, we obtain the values $E_{Tl} = 0.557[MeV]$ and $E_{Sr} = 2.335[MeV]$. From [2], we know that the energy of beta particles along the decay path of $Tl - 204$ is $0.7[MeV]$ and of $Sr - 90$ is $2.8[MeV]$, thus giving us χ^2 values of $2.932 \cdot 10^{-2}$ and $7.712 \cdot 10^{-2}$ for the energy values of $Tl - 204$ and $Sr - 90$, respectively.

Lastly, we can see in Figure (9) the count rate against the matter density for both sources (both measured data and the Beer-Lambert model), and we see that the $Tl - 204$ model seems to fit the data much better than the $Sr - 90$ model, possibly due to the differences in their decay paths and other nuclear characteristics.

3 Conclusion

In this work, we investigated a variety of phenomena related to the field of nuclear physics, using radioactive sources like $Tl - 204$, $Co - 60$, $Po - 210$, and $Sr - 90$. We found a plateau voltage of $1020[V]$ for our Geiger counter using $Tl - 204$, then measured a background radiation rate of $0.46[cps]$. We showed that the measurement distribution for $Co-60$ is Poisson-like to a high degree of confidence, and showed that the inverse-squared law for radiation is valid using $Tl-204$. Using $Po - 210$ as an alpha source, we showed that the mean range of alpha particles in air is $2.357[cm]$ ($\chi^2 = 8.136 \cdot 10^{-3}$) and their energy is $4.014[MeV]$ ($\chi^2 = 3.333 \cdot 10^{-3}$). Lastly, we found the ranges of beta particles emitted by $Tl-204$ and $Sr-90$ to be $r_{Tl} = 190.089[\frac{mg}{cm^2}]$ and $r_{Sr} = 1124.787[\frac{mg}{cm^2}]$, respectively, and found the maximal beta energies to be $E_{Tl} = 0.557[MeV]$ ($\chi^2 = 2.932 \cdot 10^{-2}$) and $E_{Sr} = 2.335[MeV]$ ($\chi^2 = 7.712 \cdot 10^{-2}$). Using the χ^2 metric for our primary error analyses, we can conclude that our experiments reflect the theories and experimental results known from the world of nuclear physics to a satisfactory extent.

References

[1] G.F. Knoll. *Radiation Detection and Measurement*. Wiley, 1977.

[2] Technion. Set of radioactive sources, 2015. https://moodle2223.technion.ac.il/pluginfile.php/367870/mod_resource/content/1/%D7%A1%D7%98%20%D7%9E%D7%A7%D7%95%D7%A8%D7%95%D7%AA%20%D7%A8%D7%93%D7%99%D7%95%D7%90%D7%A7%D7%98%D7%99%D7%91%D7%99%D7%99%D7%9D.pdf.

[3] Oregon State University. Radiation protection, 2004. https://courses.ecampus.oregonstate.edu/ne581/three/index3.htm.

Appendix A: Error Analysis

A.1 χ^2 Metric

$$\chi^2 = \sum_i \frac{(O_i - E_i)^2}{E_i}$$